EURASIAN JOURNAL OF MATHEMATICAL AND COMPUTER APPLICATIONS
ISSN 2306–6172
Volume 12, Issue 4 (2024) 67 – 74

INVERSION FORMULA FOR THE WEIGHTED CONICAL RADON TRANSFORM

Kim C., Moon S., Oh J.

Abstract The conical Radon transform, particularly relevant for Compton camera applications, maps a given function to its surface integral over a set of cones. This study focuses on the weighted conical Radon transform, obtained by incorporating a weight effect into the conical Radon transform detailed in [20]. The n-dimensional weighted conical Radon transform is first defined, following which its inversion formula is derived by expressing its projection as a convolution.

Key words: Compton camera, weight effect, conical Radon transform, inversion.

AMS Mathematics Subject Classification: 44A12; 65R10; 92C55.

DOI: 10.32523/2306-6172-2024-12-4-67-74

1 Introduction

The conical Radon transform is a mathematical operator frequently employed in various imaging techniques, particularly in Compton cameras designed for Single Photon Emission Computed tomography (SPECT). This transform maps a function to its surface integrals over a set of cones and is defined, as follows:

$$Cf(\mathbf{u},\boldsymbol{\beta},\omega)=\sin\omega\int\limits_{S^2}\int\limits_{0}^{\infty}f(\mathbf{u}+r\boldsymbol{\alpha})\delta(\boldsymbol{\alpha}\cdot\boldsymbol{\beta}-\cos\omega)\,r\mathrm{d}r\,\mathrm{d}S(\boldsymbol{\alpha}),$$

where $\mathbf{u}=(u_1,u_2,u_3)\in\mathbb{R}^3$ represents the vertex of a cone from the set, r denotes the slant height extending from $\mathbf{u}$ along the cone, $\omega\in[0,\pi]$ represents the opening angle of the cone, $\boldsymbol{\beta}\in S^2$ denotes the central axis of the cone, and $\boldsymbol{\alpha}$ corresponds to a direction vector on the surface of the cone (see Figure 1 (a)). Furthermore, S^2 represents the unit sphere in a 3-dimensional space.

SPECT is a medical imaging technique that creates 3-dimensional images by detecting gamma rays emitted from radiopharmaceuticals injected into the body. However, during SPECT, low photon counts and high noise levels typically hinder the spatial information regarding emitted gamma photons. Compton cameras help overcome these challenges [19]. In a Compton camera, emitted gamma photons first interact with a scatter detector, where they collide with electrons and undergo scattering. These scattered gamma photons then travel toward an absorption detector, where they are ultimately absorbed [1]. By analyzing the data recorded by both detectors, the energies and scattering angles of the gamma photons are determined, facilitating precise tracking of their point of emission. Importantly, in a Compton camera, all emission points of

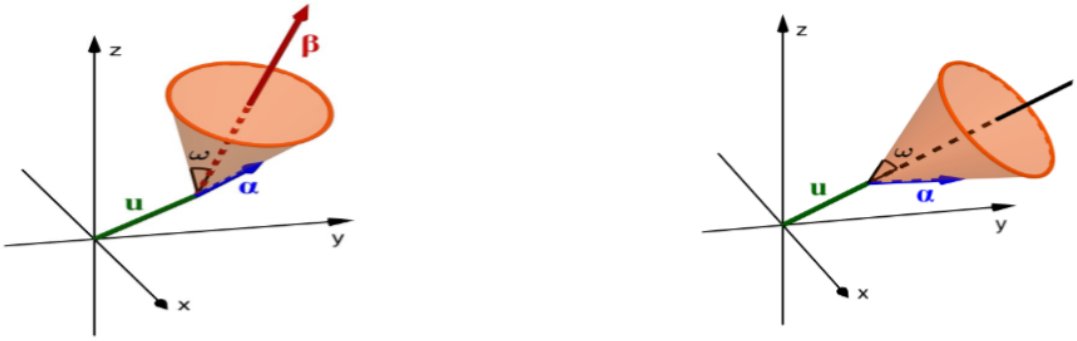

(a) $\boldsymbol{\beta} \in S^2$ (b) $\boldsymbol{\beta} = \dfrac{\mathbf{u}}{|\mathbf{u}|}$

Figure 1: Cone of integration: (a) position of vertex $\mathbf{u} \in \mathbb{R}^3$; (b) opening angle $\omega \in [0, \pi]$ and the central axis $\boldsymbol{\beta}$.

the radioactive source located on a cone-shaped surface lie along the line connecting the scattering and detextion positions. Projection data collected along such conical paths in a 3-dimensional space can be modeled using the conical Radon transform [18, 21].

The conical Radon transform can assume varying forms based on the parameters of the cones. For instance, conical Radon transforms exist for subsets of cones satisfying $\mathbf{u} \in \mathbb{R}^2 \times \{0\}$, $\boldsymbol{\beta} = \{0, 0, 1\}$, and $\omega \in (0, \frac{\pi}{2})$ [4, 15, 17]; $\mathbf{u} \in S^2$, $\boldsymbol{\beta}$ aligned orthogonal to S^2, and $\omega \in (0, \frac{\pi}{2})$ [18]; $\mathbf{u} \in \mathbb{R}^2 \times \{0\}$, $\boldsymbol{\beta} \in S^2$, and $\omega \in [0, \pi]$ [1, 13, 14]; or $\mathbf{u} \in \mathbb{R}^3$, $\boldsymbol{\beta} = \{0, 0, 1\}$, and $\omega \in (0, \frac{\pi}{2})$ [7]. For a brief review, readers are directed to [2, 21].

Among these transforms, this study particularly focuses on the conical Radon transform recently introduced in [20], where the integration of cones satisfies $\boldsymbol{\beta} = \mathbf{u}/|\mathbf{u}|$ (see Fig. 1(b)), i.e.,

$$\mathcal{C}f(\mathbf{u}, \omega) = \sin\omega \int_{S^2} \int_0^\infty f(\mathbf{u} + r\boldsymbol{\alpha})\, \delta\left(\boldsymbol{\alpha} \cdot \frac{\mathbf{u}}{|\mathbf{u}|} - \cos w\right) r\, \mathrm{d}r\, \mathrm{d}S(\boldsymbol{\alpha}). \tag{1}$$

Notably, the inversion formula for the conical Radon transform presents a challenge as it assumes that the vertices of the cone and the object being imaged lie in the same position, a scenario that is impractical in tomography, as noted in [20]. Hence, we consider the application of Compton camera technology in radiation exposure testing. For instance, when a nuclear power plant is damaged, radiation, including gamma rays, is released into the atmosphere. Because such radiation is invisible, using Compton cameras to detect gamma rays can facilitate flexible data collection without requiring precise alignment with the radioactive source, unlike conventional radiation detectors. Thus, in real-world scenarios, such Compton-camera-based radiation detectors can be moved and appropriately positioned.

In the context of SPECT, some gamma rays are absorbed as they pass through the patient's body, thus deteriorating the accuracy of the reconstructed image [10]. To compensate for this absorption effect, studies have investigated methods such as the attenuated conical Radon transform or weighted conical Radon transform [5, 9, 11,

12, 22]. Herein, the weighted conical Radon transform in n-dimensions is defined by applying a weight to the transform represented by (1) and extending it to n-dimensions.

A key contribution of this paper is that it demonstrates that the projection of the weighted conical Radon transform can be expressed as a convolution, resulting in a simplified derivation of the inversion formula. Furthermore, Section 3 presents a derivation of the inversion formula for the attenuated conical Radon transform as a special case of the weighted conical Radon transform. Moreover, subsequent sections define the weighted conical Radon transform in n-dimensions and derive its inversion formula.

2 Inversion formula for the weighted conical Radon transform

In this section, we derive the inversion formula for the n-dimensional weighted conical Radon transform, which is defined, as follows:

Definition 1. *Let $U:[0,\infty]\to\mathbb{R}$ denote a continuous function. For $\mathbf{u}\in\mathbb{R}^n$, $\omega\in[0,\pi]$ and $f\in C^\infty(\mathbb{R}^n)$ with compact support, we define the n-dimensional weighted conical Radon transform $\mathcal{C}_U$, as follows:*

$$\mathcal{C}_U f(\mathbf{u},\omega)=\sin\omega\int\limits_{S^{n-1}}\int\limits_0^\infty f(\mathbf{u}+r\boldsymbol{\alpha})\,\delta\left(\boldsymbol{\alpha}\cdot\frac{\mathbf{u}}{|\mathbf{u}|}-\cos\omega\right)U(r)\,\mathrm{d}r\,\mathrm{d}S(\boldsymbol{\alpha}).$$

To derive the inversion formula, we first express the projections of $\mathcal{C}_U f$ in the form of a convolution using the following theorem.

Theorem 2. *For $f\in C^\infty(\mathbb{R}^n)$ with compact support, we have $\int_0^\pi \mathcal{C}_U f(\mathbf{u},\omega)\mathrm{d}\omega = f*g_U(\mathbf{u})$, where $g_U(\mathbf{x})=U(|\mathbf{x}|)/|\mathbf{x}|^{n-1}$, and $\mathbf{x}\neq 0$. Furthermore, $f*g_U$ denotes the convolution of f and g_U and is defined as $f*g_U(\mathbf{u})=\int_{\mathbb{R}^n} f(\mathbf{u}-\mathbf{y})g_U(\mathbf{y})\mathrm{d}\mathbf{y}$.*

Proof. To prove this, we begin with

$$\begin{aligned}\int\limits_0^\pi \mathcal{C}_U f(\mathbf{u},\omega)\,\mathrm{d}\omega &= \int\limits_{S^{n-1}}\int\limits_0^\infty f(\mathbf{u}+r\boldsymbol{\alpha})\int\limits_0^\pi \sin\omega\,\delta\left(\boldsymbol{\alpha}\cdot\frac{\mathbf{u}}{|\mathbf{u}|}-\cos w\right)\mathrm{d}\omega\,U(r)\,\mathrm{d}r\,\mathrm{d}S(\boldsymbol{\alpha})\\ &= \int\limits_{S^{n-1}}\int\limits_0^\infty f(\mathbf{u}+r\boldsymbol{\alpha})\,U(r)\,\mathrm{d}r\,\mathrm{d}S(\boldsymbol{\alpha}) = \int\limits_{\mathbb{R}^n} f(\mathbf{u}+\mathbf{x})\frac{U(|\mathbf{x}|)}{|\mathbf{x}|^{n-1}}\,\mathrm{d}\mathbf{x},\end{aligned}$$

where we used the change of variables $\mathbf{x}\to r\boldsymbol{\alpha}$. Considering that g_U is a radial function, we have

$$\int\limits_0^\pi \mathcal{C}_U f(\mathbf{u},\omega)\,\mathrm{d}\omega = \int\limits_{\mathbb{R}^n} f(\mathbf{u}-(-\mathbf{x}))g_U(-\mathbf{x})\,\mathrm{d}\mathbf{x} = f*g_U(\mathbf{u}).$$

□

Taking the n-dimensional Fourier transform of the equation in Theorem 2, we obtain

$$\mathcal{F}\left(\int_0^\pi \mathcal{C}_U f(\cdot,\omega)\,\mathrm{d}\omega\right)(\boldsymbol{\xi}) = \mathcal{F}(f * g_U)(\boldsymbol{\xi}) = \mathcal{F}f(\boldsymbol{\xi})\mathcal{F}g_U(\boldsymbol{\xi}), \tag{2}$$

where the Fourier transform of function f is defined as

$$\mathcal{F}f(\boldsymbol{\xi}) = \int_{\mathbb{R}^n} f(\mathbf{x}) e^{-\mathrm{i}\boldsymbol{\xi}\cdot\mathbf{x}}\,\mathrm{d}\mathbf{x}.$$

The inverse Fourier transform of this result yields the inversion formula for the weighted conical Radon transform $\mathcal{C}_U f$, as follows:

Corollary 3. *If $g_U \in L^2(\mathbb{R}^n)$ and $f \in C^\infty(\mathbb{R}^n)$ with compact support, we have*

$$f(\mathbf{x}) = \mathcal{F}^{-1}\left\{\frac{1}{\mathcal{F}g_U}\,\mathcal{F}\left(\int_0^\pi \mathcal{C}_U f(\cdot,\omega)\,\mathrm{d}\omega\right)\right\}(\mathbf{x}). \tag{3}$$

For $\alpha < n$, we define the Riesz potential $\mathbf{I}^\alpha$ as $\mathbf{I}^\alpha f(\mathbf{x}) = \mathcal{F}^{-1}\left(|\cdot|^{-\alpha}\mathcal{F}f(\cdot)\right)(\mathbf{x})$.

Remark 1. *From (2), we have* $\mathcal{F}\left(\int_0^\pi \mathbf{I}^\alpha \mathcal{C}_U f(\cdot,\omega)\mathrm{d}\omega\right)(\boldsymbol{\xi}) = \mathcal{F}(\mathbf{I}^\alpha f)(\boldsymbol{\xi})\mathcal{F}g_U(\boldsymbol{\xi})$ *and*

$$f(\mathbf{x}) = \mathbf{I}^{-\alpha}\mathcal{F}^{-1}\left\{\frac{1}{\mathcal{F}g_U}\,\mathcal{F}\left(\int_0^\pi \mathbf{I}^\alpha \mathcal{C}_U f(\cdot,\omega)\,\mathrm{d}\omega\right)\right\}(\mathbf{x}).$$

3 The attenuated conical Radon transform

This section deals with cases where $U(r) = r^k e^{-\mu r}$, with $\mu \geq 0$ and k=0, 1 …, n-1. Notably, such cases are related to the conical Radon transform considering the attenuation effect. From Theorem 2 and Corollary 3, we derive the inversion formula (3) and further compute the value of $\mathcal{F}g_U$ based on the value of k. First, we define the attenuated conical Radon transform $\mathcal{C}_{k,\mu}$, as follows:

$$\mathcal{C}_{k,\mu} f(\mathbf{u},\omega) = \sin\omega \int_{S^{n-1}} \int_0^\infty f(\mathbf{u} + r\boldsymbol{\alpha})\,\delta\left(\boldsymbol{\alpha}\cdot\frac{\mathbf{u}}{|\mathbf{u}|} - \cos\omega\right) r^k e^{-\mu r}\,\mathrm{d}r\,\mathrm{d}S(\boldsymbol{\alpha}).$$

Subsequently, using Theorem 2 and Corollary 3, we obtain

$$\int_0^\pi \mathcal{C}_{k,\mu} f(\mathbf{u},\omega)\,\mathrm{d}\omega = f * g_{k,\mu}(\mathbf{u}) \quad\text{and}\quad f(\mathbf{x}) = \mathcal{F}^{-1}\left\{\frac{1}{\mathcal{F}g_{k,\mu}}\,\mathcal{F}\left(\int_0^\pi \mathcal{C}_{k,\mu} f(\cdot,\omega)\,\mathrm{d}\omega\right)\right\}(\mathbf{x}),$$

where $f \in C^\infty(\mathbb{R}^n)$ with compact support and $g_{k,\mu}(\mathbf{x}) = e^{-\mu|\mathbf{x}|}/|\mathbf{x}|^{n-k-1}$, $\mathbf{x} \neq 0$. We then compute $\mathcal{F}g_{k,\mu}$, as follows: [6, eq. (7.38) on page 247]

$$\mathcal{F}g_{k,\mu}(\boldsymbol{\xi}) = (2\pi)^{n/2} \int_0^\infty e^{-\mu r} r^{1-n+k} (r|\boldsymbol{\xi}|)^{1-(n/2)} J_{(n/2)-1}(r|\boldsymbol{\xi}|) r^{n-1}\,\mathrm{d}r.$$

3.1 $k = n - 2$

The attenuated conical Radon transform is defined as

$$\mathcal{C}_{n-2,\mu} f(\mathbf{u}, \omega) = \sin\omega \int_{S^{n-1}} \int_0^\infty f(\mathbf{u} + r\boldsymbol{\alpha})\, \delta\left(\boldsymbol{\alpha} \cdot \frac{\mathbf{u}}{|\mathbf{u}|} - \cos\omega\right) r^{n-2} e^{-\mu r}\, \mathrm{d}r\, \mathrm{d}S(\boldsymbol{\alpha}).$$

Using this definition, we obtain

$$\begin{aligned}
\mathcal{F} g_{n-2,\mu}(\boldsymbol{\xi}) &= (2\pi)^{n/2} \int_0^\infty r^{-1} e^{-\mu r} (r|\boldsymbol{\xi}|)^{1-(n/2)} J_{(n/2)-1}(r|\boldsymbol{\xi}|) r^{n-1}\, \mathrm{d}r \\
&= (2\pi)^{n/2} |\boldsymbol{\xi}|^{(1-n)/2} \int_0^\infty r^{(n-3)/2} e^{-\mu r} J_{(n/2)-1}(r|\boldsymbol{\xi}|)(r|\boldsymbol{\xi}|)^{1/2}\, \mathrm{d}r \\
&= (2\pi)^{n/2} |\boldsymbol{\xi}|^{(1-n)/2} \big\{ 2^{(n/2)-1} \pi^{-1/2} \Gamma((n-1)/2) |\boldsymbol{\xi}|^{(n-1)/2} (\mu^2 + |\boldsymbol{\xi}|^2)^{(1-n)/2} \big\},
\end{aligned}$$

where the final step uses the following equation [3, eq. (5) on page 29]:

$$\int_0^\infty r^{\nu-1/2} e^{-\mu r} J_\nu(r|\boldsymbol{\xi}|)(r|\boldsymbol{\xi}|)^{1/2}\, \mathrm{d}r = 2^\nu \pi^{-1/2} \Gamma(\nu + 1/2) |\boldsymbol{\xi}|^{\nu+1/2} (\mu^2 + |\boldsymbol{\xi}|^2)^{-\nu-1/2}.$$

Thus, we have

$$\mathcal{F} g_{n-2,\mu}(\boldsymbol{\xi}) = 2^{n-1} \pi^{(n-1)/2} \Gamma((n-1)/2)) (\mu^2 + |\boldsymbol{\xi}|^2)^{(1-n)/2}. \tag{4}$$

3.2 $k = n - 1$ and $k = 0$

Similar to the approach detailed in Section 3.1, we obtain $\mathcal{F} g_{n-1,\mu}$, as follows:

$$\begin{aligned}
\mathcal{F} g_{n-1,\mu}(\boldsymbol{\xi}) &= (2\pi)^{n/2} \int_0^\infty e^{-\mu r} (r|\boldsymbol{\xi}|)^{1-(n/2)} J_{(n/2)-1}(r|\boldsymbol{\xi}|) r^{n-1}\, \mathrm{d}r \\
&= (2\pi)^{n/2} |\boldsymbol{\xi}|^{(1-n)/2} \int_0^\infty r^{(n-1)/2} e^{-\mu r} J_{(n/2)-1}(r|\boldsymbol{\xi}|)(r|\boldsymbol{\xi}|)^{1/2}\, \mathrm{d}r \\
&= 2^n \pi^{(n-1)/2} \Gamma((n+1)/2)) \mu (\mu^2 + |\boldsymbol{\xi}|^2)^{(-1-n)/2},
\end{aligned}$$

where the final step uses the following equation [3, eq. (4) on page 29]:

$$\int_0^\infty r^{\nu+1/2} e^{-\mu r} J_\nu(r|\boldsymbol{\xi}|)(r|\boldsymbol{\xi}|)^{1/2}\, \mathrm{d}r = 2^{\nu+1} \pi^{-1/2} \Gamma(\nu + 3/2) \mu |\boldsymbol{\xi}|^{\nu+1/2} (\mu^2 + |\boldsymbol{\xi}|^2)^{-\nu-3/2}.$$

We also derive $\mathcal{F} g_{0,\mu}$ for case $k = 0$, as follows:

$$\begin{aligned}
\mathcal{F} g_{0,\mu}(\boldsymbol{\xi}) &= (2\pi)^{n/2} \int_0^\infty e^{-\mu r} (r|\boldsymbol{\xi}|)^{1-(n/2)} J_{(n/2)-1}(r|\boldsymbol{\xi}|)\, \mathrm{d}r \\
&= (2\pi)^{n/2} |\boldsymbol{\xi}|^{(1-n)/2} \int_0^\infty r^{(1-n)/2} e^{-\mu r} J_{(n/2)-1}(r|\boldsymbol{\xi}|)(r|\boldsymbol{\xi}|)^{1/2}\, \mathrm{d}r \\
&= (2\pi)^{n/2} |\boldsymbol{\xi}|^{1-n/2} (\mu^2 + |\boldsymbol{\xi}|^2)^{n/4-1} \mathrm{P}_{1-n/2}^{1-n/2} \left[\mu (\mu^2 + |\boldsymbol{\xi}|^2)^{-1/2} \right],
\end{aligned}$$

where P_ν^λ denotes the Legendre function of the first kind and the final step uses the following equation [3, eq.(6) on p. 29]:

$$\int_0^\infty r^{a-3/2} e^{-\mu r} J_\nu(r|\boldsymbol{\xi}|)(r|\boldsymbol{\xi}|)^{1/2}\,\mathrm{d}r = |\boldsymbol{\xi}|^{1/2}(\mu^2+|\boldsymbol{\xi}|^2)^{-a/2}\Gamma(a+\nu)\mathrm{P}_{a-1}^{-\nu}\left[\mu(\mu^2+|\boldsymbol{\xi}|^2)^{-1/2}\right].$$

3.3 $n = 2$ and 3 with $\mu = 0$ and $k = n - 2$

This subsection deals with the inversion formula for the 2-and 3-dimensional conical Radon transforms (i.e., $\mu = 0$). Based on Corollary 3, we have

$$f(\mathbf{x}) = \mathcal{F}^{-1}\left\{\frac{1}{\mathcal{F}g_{n-2,0}}\,\mathcal{F}\left(\int_0^\pi \mathcal{C}_{n-2,0}f(\cdot,\omega)\,\mathrm{d}\omega\right)\right\}(\mathbf{x}),$$

where $\mathcal{F}g_{n-2,0}(\boldsymbol{\xi}) = 2^{n-1}\pi^{(n-1)/2}\Gamma((n-1)/2))|\boldsymbol{\xi}|^{(1-n)}$ (see [8, p. 363] or substituting $\mu = 0$ in (4)). Thus, the inversion formulas for $n = 2$ and $n = 3$ are respectively expressed as,

$$f(\mathbf{x}) = \frac{1}{2\pi}\mathcal{F}^{-1}\left\{|\cdot|\,\mathcal{F}\left(\int_0^\pi \mathcal{C}_{0,0}f(\cdot,\omega)\,\mathrm{d}\omega\right)\right\}(\mathbf{x})$$

(which is the same as (4) in [20]) and

$$f(\mathbf{x}) = \frac{1}{4\pi}\mathcal{F}^{-1}\left\{|\cdot|^2\,\mathcal{F}\left(\int_0^\pi \mathcal{C}_{1,0}f(\cdot,\omega)\,\mathrm{d}\omega\right)\right\}(\mathbf{x}) = \frac{1}{4\pi}\int_0^\pi \Delta_{\mathbf{u}}\mathcal{C}_{1,0}f(\mathbf{u},\omega)\,|_{\mathbf{u}=\mathbf{x}}\;\mathrm{d}\omega.$$

3 Conclusion

This paper extends the n-dimensional conical Radon transform detailed in [20] by incorporating a weight effect. Specifically, the projection of the weighted conical Radon transform is expressed as a convolution with a specific radial function. Based on this result, the corresponding inversion formula is derived. Developing and implementing simulations based on this inversion formula present significant challenges and important topics for our future research.

Acknowledgement

This work was supported by the National Research Foundation of Korea (NRF-2022R1C1C1003464 and RS-2023-00217116).

References

[1] Allmaras M., Darrow D.P., Hristova Y., Kanschat G., Kuchment P., *Detecting small low emission radiating sources*, Inverse Problems and Imaging, 7(1):47-79, 2013

[2] Ambartsoumian G., Latifi Jebelli M.J., *The V-line transform with some generalizations and cone differentiation*, Inverse Problems, 35(3):034003, 2019.

[3] Bateman H., Erdélyi A. , Magnus W., Oberhettinger F., *Tables of integral transforms (Vol. 2)*, New York: McGraw-Hill, 1954.

[4] Cebeiro J., Morvidone M., Nguyen M.K., *Back-projection inversion of a conical Radon transform*, Inverse Problems in Science and Engineering, 24(2):328-352, 2016.

[5] Duy N. N., *Analysis of the weighted conical Radon transform*, Journal of Physics Communications, 8(3):035004, 2024.

[6] Folland G. B., *Fourier analysis and its applications (Vol. 4)*, American Mathematical Soc, 2009.

[7] Gouia-Zarrad R., Ambartsoumian G., *Exact inversion of the conical Radon transform with a fixed opening angle*, Inverse Problems, 30(4):045007, 2014).

[8] Gelfand I. M., Shilov G. E., *Generalized Functions, vol. 1*, New York: Academic Press, 1964.

[9] Gouia-Zarrad R., Moon S., *Inversion of the attenuated conical Radon transform with a fixed opening angle*, Mathematical Methods in the Applied Sciences, 41(18): 8423-8431, 2018.

[10] Haltmeier M., Moon S., Schiefeneder D., *Inversion of the attenuated v-line transform with vertices on the circle*, IEEE Transactions on Computational Imaging, 3(4):853-863, 2017.

[11] Haltmeier M., Schiefeneder D., *Variational regularization of the weighted conical Radon transform*, Inverse problems, 34(12):124009, 2018).

[12] Jeon G., Moon S., *Singular value decomposition of the attenuated conical Radon transform with a fixed central axis and opening angle*, Integral Transforms and Special Functions, 32(10):812-822, 2021.

[13] Jung C., Moon S., *Inversion formulas for cone transforms arising in application of Compton cameras*, Inverse Problems, 31(1): 015006, 2015.

[14] V. Maxim, M. Frandes, and R. Prost, *Analytical inversion of the Compton transform using the full set of available projections*, Inverse Problems, 25(9):095001, 2009.

[15] Moon S., *On the determination of a function from its conical Radon transform with a fixed central axis*, SIAM Journal on Mathematical Analysis, 48(3):1833-1847, 2016.

[16] Moon S., Haltmeier M., *The conical Radon transform with vertices on triple line segments*, Inverse Problems, 36(11):115005, 2020.

[17] Nguyen M. K. , Truong T. T., Grangeat P., *Radon transforms on a class of cones with fixed axis direction*, Journal of Physics A: Mathematical and General, 38(37): 8003-8015, 2005.

[18] Schiefeneder D., Haltmeier M., *The Radon transform over cones with vertices on the sphere and orthogonal axes*, SIAM Journal on Applied Mathematics, 77(4): 1335-1351, 2017.

[19] Singh M., *An electronically collimated gamma camera for single photon emission computed tomography. Part I: Theoretical consideration and design criteria*, Medical Physics, 10(4): 421-427, 1983.

[20] Tarpau C., Cebeiro J., Nguyen M. K., Rollet G., Dumas L., *An analytic inversion formula for a Radon transform on a class of cones*, Eurasian Journal of Mathematical and Computer Applications, 10(3): 73-83, 2022.

[21] Terzioglu F., Kuchment P., Kunyansky L., *Compton camera imaging and the cone transform: a brief overview*, Inverse Problems, 34(5): 054002, 2018.

[22] Zhang Y., *Recovery of singularities for the weighted cone transform appearing in Compton camera imaging*, Inverse Problems, 36(2):025014, 2020.

Chaeyoon Kim,
College of Natural Sciences,
Kyungpook National University,
Daegu 41566, Republic of Korea

Sunghwan Moon,
College of Natural Sciences,
Kyungpook National University,
Daegu 41566, Republic of Korea,
Email: sunghwan.moon@knu.ac.kr

Jiyoung Oh,
Kyungpook National University,
Daegu 41566, Republic of Korea,
Email: dhwldud0124@knu.ac.kr

Received 25.06.2024, Revised 13.08.2024, Accepted 14.08.2024